Journal of Inflammation Research

Dovepress
Taylor & Francis Group

Open Access Full Text Article

ORIGINAL RESEARCH

Remote Continuous Microinjury-Triggered Cytokines Facilitate Severe Diabetic Foot Ulcer Healing via the Ras/Raf/MEK/ERK Pathway

Xiajie Huang[1,2,*], Jie Liu[1,*], Xiaomei Wu[1], Yangzhou Mo[1], Xiping Luo[1], Yongge Yang[1], Chaoquan Yang[1], Xinyun Liang[1], Rongyuan Liang[1], Yeping Chen[1], Zezhen Fan[1], William Lu[3], Yan Chen[1], Qikai Hua[1]

[1]Department of Bone and Joint Surgery, The First Affiliated Hospital of Guangxi Medical University, Nanning, People's Republic of China; [2]Collaborative Innovation Centre of Regenerative Medicine and Medical BioResource Development and Application Co-Constructed by the Province and Ministry, Guangxi Medical University, Nanning, People's Republic of China; [3]Department of Orthopaedics and Traumatology, The University of Hong Kong, Hong Kong, People's Republic of China

*These authors contributed equally to this work

Correspondence: Yan Chen; Qikai Hua, Department of Bone and Joint Surgery, The First Affiliated Hospital of Guangxi Medical University, Nanning, People's Republic of China, Email cy003@connect.hku.hk; hqk100@yeah.net

Purpose: Microinjury can trigger in situ tissue repair. Bone transport consists of continuous microinjuries/microfracture and induces bone formation and angiogenesis. Tibial cortex transverse transport (TTT) was found to promote angiogenesis at the foot and the healing of diabetic foot ulcers (DFUs). However, the underlying mechanism remains largely unknown.

Methods: We divided 72 Sprague-Dawley rats with DFUs into the control, sham, and TTT groups. Wound measurement and histology were performed to evaluate the wound healing processes. Enzyme-linked immunosorbent assay, flow cytometry, immunohistochemistry, and Western Blot were used to assess angiogenesis and the activity of endothelial progenitor cells (EPCs) and the Ras/Raf/MEK/ERK signaling pathway.

Results: We found accelerated wound healing, improved epidermal continuity, and increased dermal thickness in the TTT group than the control and the sham groups. Higher levels of serum TGF-β1, PDGF-BB, and VEGF were detected in the TTT group. These changes were in parallel with the expression of TGF-β1, PDGF-BB, and VEGF in the foot wounds and the frequency of EPCs in both bone marrow and peripheral circulation, which implied that the secreted TGF-β1, PDGF-BB, and VEGF promote proliferation and migration of EPCs to the foot wounds. The expression of $CD31^+$ cells, SMA-α^+ cells, and the Ras/Raf/MEK/ERK pathway was higher in the TTT group than in the control and sham groups.

Conclusion: The findings showed that TTT enhanced the production of growth factors that in turn activated EPC proliferation and migration through the Ras/Raf/MEK/ERK pathway, ultimately contributing to angiogenesis and DFU healing. Based on these findings, we proposed a theory that remote continuous microinjuries can trigger the repair of target tissues (ie, microinjury-induced remote repair, MIRR). Future studies are needed to validate this theory.

Keywords: microinjury, bone transport, tibial cortex transverse transport, diabetic foot ulcer, endothelial progenitor cells, Ras/Raf/MEK/ERK signaling pathway

Introduction

Injury can trigger in situ tissue repair.[1] Furthermore, microinjury can even mediate localized tissue regeneration without causing severe trauma or scarring.[2] Bone transport, or distraction osteogenesis, is a surgical technique in which an osteotomy is performed followed by gradual distraction.[3–5] The procedure of bone transport is composed of three sequential phases including latency, distraction, and consolidation.[3–5] During the latency phase, new bone is gradually formed (ie, fracture healing) at the osteotomy site. Nevertheless, this newly formed bone is disrupted (ie, microfracture) by the distraction, followed by new bone formation again until the next distraction.[3–6] Thus, the bone transport process

Received: 9 September 2024
Accepted: 25 January 2025
Published: 5 February 2025

comprises many "microfracture-bone healing-microfracture" cycles, or continuous microinjuries (ie, microfractures).[3–6] Importantly, new bone formation in bone transport[3,4,7,8] is accompanied by angiogenesis in both the bone and the surrounding tissues.[9–14] Consequently, this technique has been proposed for the treatment of localized ischemic diseases.[3]

As the world's population is aging, the incidence of diabetes mellitus is increasing, from approximately 10.5% (536.6 million people) in 2021 to an estimated 12.2% (783.2 million) by 2045 among individuals aged 20–79.[15,16] A critical consequence of diabetes is foot complications.[17] Notably, 19% to 34% of diabetic individuals develop a foot ulcer during their lifetime.[18] Despite the availability of traditional conservative and surgical approaches, management of diabetic foot ulcers (DFUs) remains a challenge.[18,19] Around 20% of patients with DFUs require lower-extremity amputation, and 10% of these patients die within the first year following their initial diagnosis.[18,19]

DFUs are attributable to a number of risk factors, among which peripheral arterial disease is one of the major ones. Arteriosclerosis obliterans can result in localized ischemia and hypoxia, leading to necrosis of tissues such as the skin, fascia, muscles, nerves, and bones.[20,21] Consequently, a new surgical technique, tibial cortex transverse transport (TTT) which involves a partial tibial corticotomy followed by transverse distraction, has been developed by our and other groups for the treatment of severe DFUs.[5,22,23] Studies found that TTT enhanced angiogenesis at the foot, ultimately resulting in DFU healing.[5,22,23] Because TTT can be considered a procedure with continuous microinjuries (microfractures), here, we proposed that continuous microinjuries can trigger the intrinsic repair ability of the body, leading to not only in situ but also remote target tissue repair - that is, the theory of "microinjury-induced remote repair (MIRR)". Nevertheless, this theory needs further validation.

Angiogenesis is associated with the proliferation and differentiation of endothelial progenitor cells (EPCs).[24] EPCs are primarily found in the bone marrow cavity and can be activated by growth factors to proliferate and migrate into the peripheral blood.[24] EPCs can further reach the injury site through circulation and contribute to localized angiogenesis and wound healing.[25–27] Previous studies indicated that EPCs may be involved in the healing of DFUs treated using TTT.[28] However, the specific function of EPCs in DFU management utilizing TTT remains unclear.

Among the numerous intracellular signaling pathways that mediate angiogenesis, the Ras/Raf/MEK/ERK pathway is a critical one.[29] This pathway is closely linked to the regulation of vascular endothelial growth factor (VEGF) and VEGF receptor 2 (VEGFR2).[30] The activation of the Ras/Raf/MEK/ERK pathway regulates cell proliferation and differentiation and transmits extracellular signals to the nucleus through a series of protein kinase cascades.[31,32] Prior studies showed that the upregulation of the Ras/Raf/MEK/ERK pathway enhanced DFU healing.[33] However, the exact effect of the Ras/Raf/MEK/ERK pathway on angiogenesis and DFU is to be elucidated.

Thus, in this study, we investigated the healing process of ischemic DFUs after TTT, together with changes in angiogenesis at the foot wound and the activity of EPCs and the Ras/Raf/MEK/ERK pathway. We hypothesized that TTT-trigged growth factors mediated angiogenesis at the DFU and facilitated wound healing via activation of EPCs through the Ras/Raf/MEK/ERK pathway. The results of the study could support the theory of remote continuous microinjury-induced repair.

Materials and Methods

Animals and Study Design

In this study, we obtained 72 male Sprague-Dawley rats, each 12 weeks old, with an average weight of 380 grams and a standard deviation of 11.2 grams, from the Animal Center of Guangxi Medical University. After diabetes induction (as described in Diabetes Induction below), all animals were randomly assigned to the control, the sham, and the TTT groups (Figure 1).[34] In the control group, we performed the femoral artery ligation to induce limb ischemia, followed by the creation of a wound on the dorsum of the foot (as described in the Surgical protocol below). In the TTT group, an additional tibial corticotomy and transverse distraction were conducted (as described in the Surgical protocol below). The sham group underwent a corticotomy without the transverse movement of the osteotomized cortex. In contrast, the control group underwent neither corticotomy nor distraction (as described in the Surgical Protocol below) (Figure 1). Our animal study was conducted according to the National Institutes of Health guidelines and approved by the Animal Ethics Committee of The First Affiliated Hospital of Guangxi Medical University (Approval Reference: 2022-D170-01).

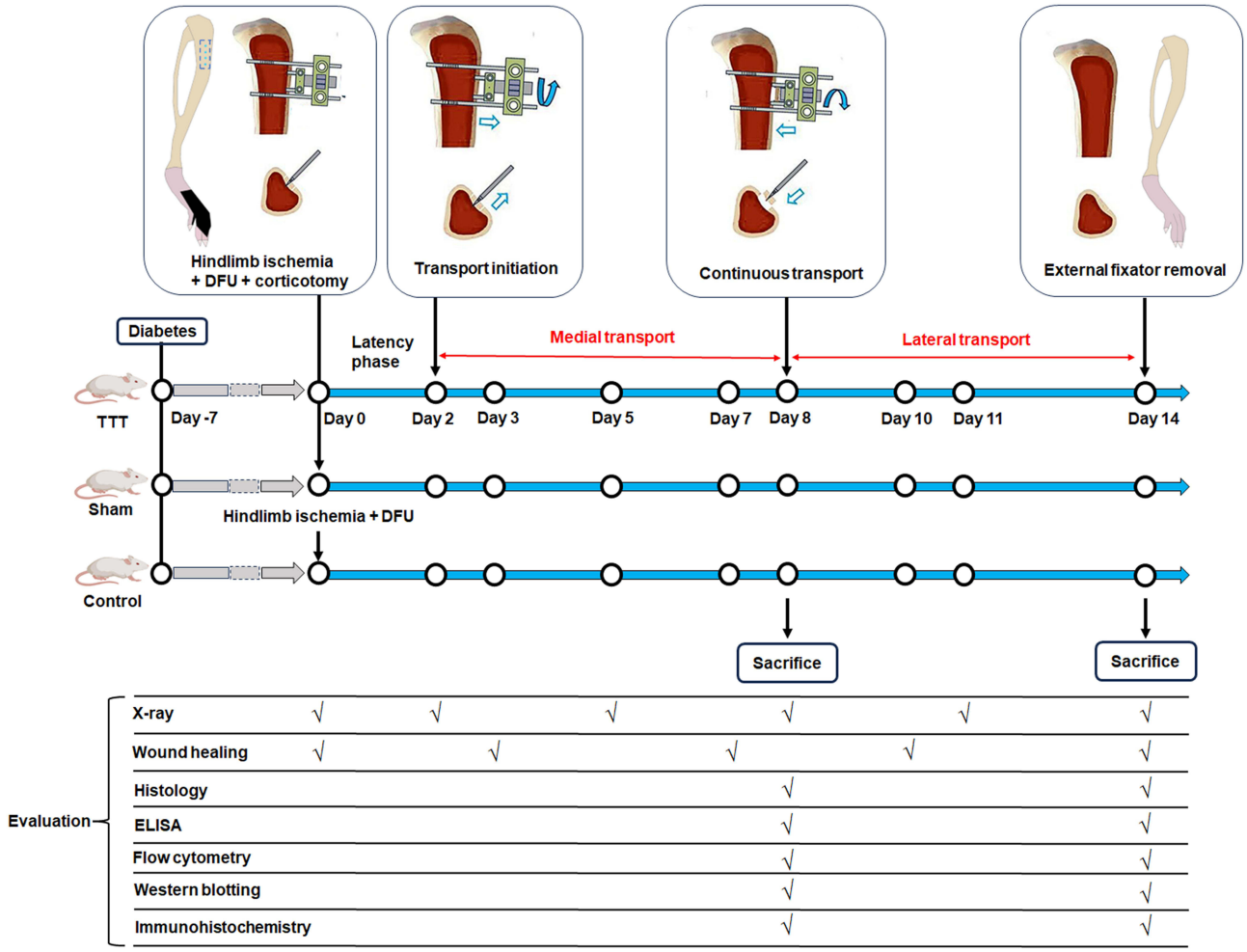

Figure 1 The study design and the evaluation at each stage. Seven days after diabetes induction, the ligation of the femoral artery and the creation of a DFU were performed in the control group. In addition, a tibial corticotomy was performed, an external distractor was attached, and the bone segment was transversely distracted in the TTT group. The distraction period consisted of a 6-day medial transport and a 6-day lateral transport. After this, the bone fragment returned to its original position as confirmed using X-ray, and the external distractor was removed. The procedures of the sham group were the same as those of the TTT group but the bone segment was not distracted.

Abbreviations: DFU, diabetic foot ulcer; TTT, tibial cortex transverse transport; ELISA, enzyme-linked immunosorbent assay; X-ray, radiographs.

Diabetes Induction

Diabetes was induced in the rats as described before.[34] Briefly, streptozotocin was administered intraperitoneally at a dose of 55 mg/kg (S8050, Solarbio), dissolved in a sodium citrate solution (0.01 M, pH 4.3).[35] Three days later, blood glucose levels were assessed using the Accutrend sensor (Roche Biochemicals, Mannheim, Germany). Diabetes was confirmed with blood glucose levels over 250 mg/dL (13.9 mmol/L).[36]

Surgical Protocol

Seven days after diabetes induction, surgical procedures were initiated with the animals under anesthesia induced by 35 mg/kg of 2% sodium pentobarbital.[34,37] Hindlimb ischemia was induced by ligating the femoral artery (Figure 2A). Then, a cortical osteotomy on the medial side of the tibia was performed and the distraction system including fixation pins and distraction pins was installed (Figure 2B–F).[34] Finally, a wound was created on the dorsum of the foot by excising a section of full-thickness skin and subcutaneous tissue (2 cm by 1 cm) (Figure 2G–I).[34] Immediate post-operative X-rays were taken to confirm the positions of the osteotomized cortex and the fixation and distraction pins (Figure 2J).

https://doi.org/10.2147/JIR.S493505

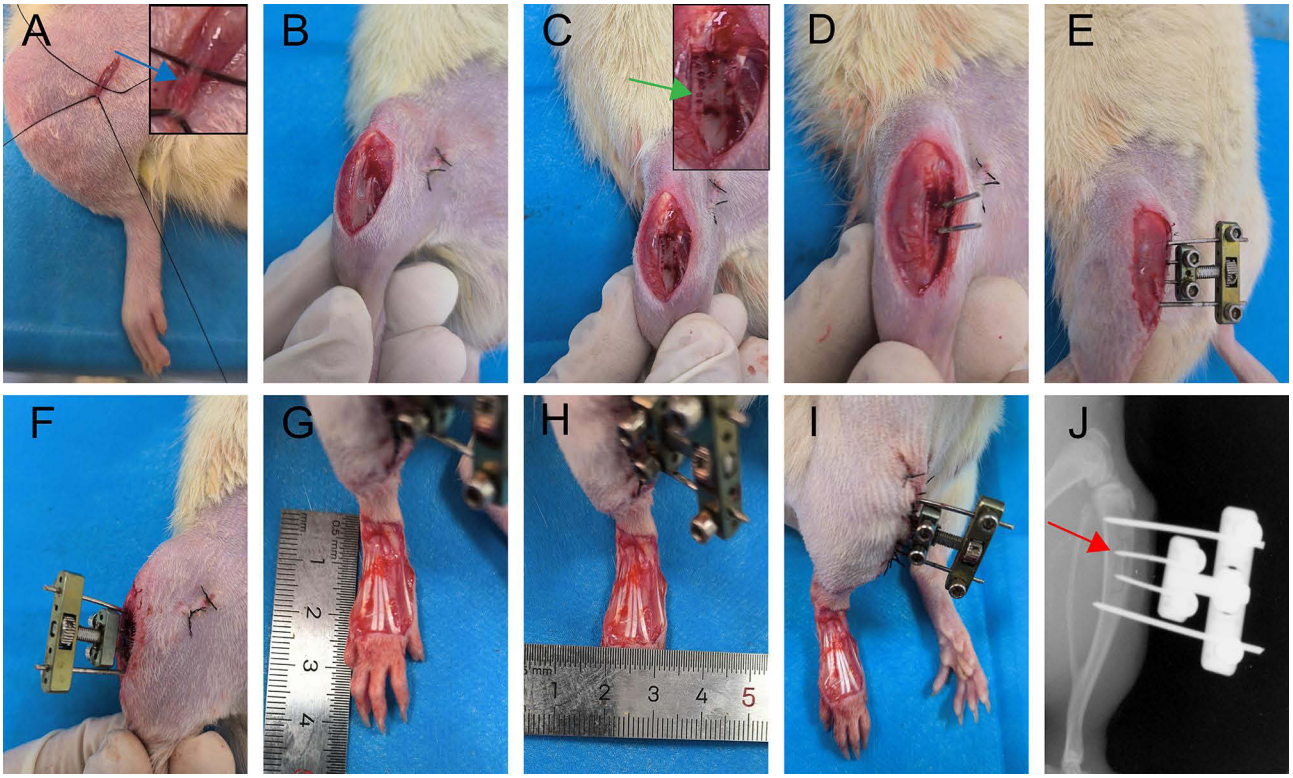

Figure 2 Surgical procedure. (**A**) Seven days after diabetes induction, the femoral artery (blue arrow) was ligated to induce hindlimb ischemia. The procedure includes isolating the femoral artery from the surrounding tissues, securely tying off both ends with sutures, then cutting the artery in the middle, and finally suturing the incision closed. (**B**) The proximal medial tibia was exposed. (**C**) Multiple consecutive single cortical holes (green arrows) were drilled to create a cortical osteotomy (10 mm high, 5 mm wide) under the guidance of an external distractor. Two 0.8-mm pins were inserted into the osteotomy fragment to distract the bone fragments, while two 1.0-mm pegs were placed into the tibial shaft to secure the customized external distractor. The cortical holes were connected using a small bone chisel to separate the cortex from the tibial shaft. (**D**–**F**) The external fixator was assembled, and the incision was closed. (**G**–**I**) The entire skin and subcutaneous tissue on the dorsum of the foot were excised to create a rectangular wound (2 cm long and 1 cm wide). (**J**) Postoperative X-rays were taken to verify the corticotomy (indicated by the red arrow) and the position of the Kirschner wires.

Tibial Cortex Transverse Distraction

Following a two-day latency period, tibial cortex transverse transport was initiated in the TTT group. The distraction was performed at a rate of 0.1 mm every 12 hours by turning the nuts of the distraction nail. The distraction phase comprises a six-day medial distraction and a six-day lateral transport. The total displacement was 1.2 mm (Figure 3). The osteotomized cortex achieved its maximum displacement of 0.6 mm at day 8 and returned to its initial position at day 14, and was then removed (Figure 3).

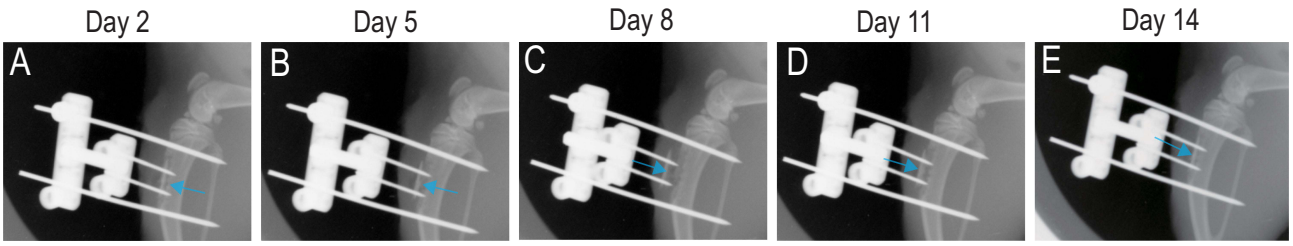

Figure 3 These postoperative X-rays illustrate the progression of TTT. (**A**) Before initiating the transverse transport, the position of the osteotomy piece (indicated by the arrow) and the external distractor were confirmed. (**B**) After 3 days of medial transport, the displacement of the corticotomized fragment became apparent. (**C**) By day 8, the corticotomized fragment had reached its maximum displacement. (**D** and **E**) This was followed by 6 days of lateral transport, after which, at day 14, the corticotomized fragment returned to its original position, and the external distractor was removed.

Radiographs

Radiographs were taken immediately after the surgery and at days 2, 5, 8, 11, and 14, respectively, to verify the positions of the osteotomized cortex and the pins (Figure 1).

Wound Healing Assessment

To assess wound healing, digital images of the wounds were captured at days 0, 3, 7, 10, and 14, respectively. Each image included a reference scale for standardized measurement calibration. Wound boundaries were manually delineated by a trained technician using ImageJ software (NIH, USA),[38] based on clear anatomical landmarks visible in the digital photographs. The wound area was reported as a percentage of the original size at each time point, calculated by determining the ratio of the remaining wound area to the initial wound area at day 0.

Histology

Skin defect samples encompassing the entire affected area were collected at day 8 and day 14, respectively, by excising the entire wound area, including a 2–3 mm margin of surrounding healthy skin, down to the underlying muscle layer, using a sterile surgical scalpel. These samples were then fixed in 10% neutral buffered formalin for 24 hours, dehydrated through a graded series of ethanol, cleared in xylene, and embedded in paraffin. Five-micron-thick sections were cut using a microtome and subsequently mounted on glass slides. Hematoxylin and Eosin (H&E) staining was performed according to standard protocols.[39,40] Briefly, sections were deparaffinized, rehydrated through a graded alcohol series, stained with hematoxylin, differentiated in acid alcohol, blued in alkaline water, counterstained with eosin, dehydrated, and mounted.[39,40] Dermal thickness was measured by identifying the boundaries between the epidermis and the subcutaneous layer using the ImageJ software.[41] Three randomly selected locations per sample were analyzed. All assessments were performed by a single evaluator who was unaware of the specimen's condition.

Enzyme-Linked Immunosorbent Assay (ELISA)

Peripheral blood was collected from the heart via sterile fine needle aspiration under anesthesia at day 8 and day 14, respectively. Blood samples were allowed to clot at room temperature followed by centrifugation at 2000 rpm for 10 minutes to separate the serum.[34] Following serum collection, TGF-β1, VEGF, and PDGF-BB levels were quantified using ELISA kits according to the manufacturer's protocols (VEGF ELISA kit, EK383/2, MultiSciences; PDGF-BB ELISA kit, EK9137, MultiSciences; TGF-β1 ELISA kit, EK981, MultiSciences).

Flow Cytometry

Phosphate Buffered saline (PBS) without calcium and magnesium, supplemented with 2% heat-inactivated bovine serum, was drawn into a 2.5 mL syringe. The syringe was inserted into the bone marrow cavity and the bone marrow was flushed out from the tibia until the tibia appeared white or transparent. The cells were subsequently processed by gently drawing them through a needle of 25-gauge, followed by straining through a nylon mesh with a pore size of 70 microns to achieve a single-cell suspension. For peripheral blood samples, blood was collected from the orbital area and transferred into anticoagulant tubes (EDTA). About 300 microliters of this blood were mixed with 2 mL of a 1x red blood cell lysis solution (R1010, Solarbio), and after lysing for 5 minutes, the sample was washed with PBS containing 2% BSA at 1000 rpm for 5 minutes. The cells were resuspended in a PBS solution free from calcium and magnesium, then EPC-specific antibodies (anti-CD34, sc-7324AF488, Santa Cruz; anti-CD133, sc-365537PE, Santa Cruz; and anti-VEGFR2, sc-6251AF647, Santa Cruz) were added, and the mixture was incubated at room temperature for 15 minutes. All antibody concentrations and doses were used according to the reagent instructions. The sample was washed with PBS containing 2% BSA at 1000 rpm for 5 minutes, and the cells were resuspended in a PBS solution free from calcium and magnesium. Finally, the cell suspension was immediately analyzed using a flow cytometer (FACSVerse, BD) to determine the presence and quantity of EPCs (Supplementary Figure 1).

Western Blot

Foot ulcer tissues were excised using a sterile scalpel, snap-frozen in liquid nitrogen, and stored at −80°C. Prior to analysis, the samples were homogenized in RIPA buffer (200uL per 20 mg tissue, K1020, APExBIO, USA) using a mechanical homogenizer on ice. SDS-PAGE Sample Loading Buffer (P0015L, Beyotime, China) was then added. The resulting proteins were separated by 10% SDS-PAGE under constant voltage to resolve proteins based on their molecular weight. Following electrophoresis, the proteins were transferred onto PVDF membranes (Millipore, USA) using a semi-dry transfer system, ensuring efficient protein immobilization for subsequent analysis. Then, the membranes were blocked using skimmed milk for 1 hour at room temperature, followed by incubation with primary antibodies overnight at 4°C: anti-ERK1/2 (11257-1-AP, dilution 1:3000; Proteintech), anti-p-ERK1/2 (28733-1-AP, dilution 1:1000; Proteintech), and anti-α-tubulin (11224-1-AP, dilution 1:7000; Proteintech). Subsequently, the membranes were incubated for 1 hour with Goat anti-Rabbit IgG (H+L) Secondary Antibody, HRP (31460, Invitrogen, USA). Protein bands were detected using the ECL Chemiluminescent Substrate Detection Kit (K1129, APExBIO, USA), and their intensities were quantified relative to internal reference bands using ImageJ software (NIH, USA).[38] Graphs were generated using GraphPad Prism version 9.5.1 for Windows (GraphPad Software, San Diego, California, USA, www.graphpad.com).

Immunohistochemistry

Immunohistochemistry was performed as described.[39,42] Briefly, sections underwent heat-induced antigen retrieval in citrate buffer, followed by incubation with the primary antibodies overnight: Anti-SMA-α (GB111364, dilution 1:500; Servicebio), anti-CD31 (GB11063-2, dilution 1:100; Servicebio), anti-PDGF-BB (GB11261, dilution 1:300; Servicebio), anti-VEGF (26157-1-AP, dilution 1:200; Proteintech), anti-TGF-β1 (21898-1-AP, dilution 1:200; Proteintech), anti-C-RAF (AF6062, dilution 1:100; Affinity), anti-Ras (AF0247, dilution 1:100; Affinity), anti-ERK1/2 (11257-1-AP, dilution 1:200; Proteintech), and anti-p-ERK1/2 (28733-1-AP, dilution 1:100; Proteintech). Then, horseradish peroxidase-labeled goat anti-rabbit secondary antibodies (GB23303, 1:200 dilution; Servicebio) were added and incubated for 60 min. Substrate diaminobenzidine (DAB) (Vector Lab, California, USA) was used to develop color. Images were captured followed by quantification of the number of positive stained cells as previously described.[34] All tissue samples were parallel processed and identical reagents and protocols were used for the staining.

Statistical Methods

Data are presented as mean ± standard deviation, and normality was assessed using the Shapiro–Wilk test. Group differences were analyzed using one-way analysis of variance (ANOVA), and where statistically significant results were found, post hoc tests (Tukey's multiple comparison test) were applied.[43] The significance level was set at $\alpha < 0.05$. All statistical analyses were conducted using GraphPad Prism software (version 9.5.1, USA).

Results

TTT Enhanced DFU Healing

Radiographs taken at days 2, 5, 8, 11, and 14, respectively, confirmed the locations of the osteotomized cortex and the distraction system (Figure 3). The cortectomy site showed no tibial fractures or Kirschner wire displacement. Signs of infections that presented as cellulitis or suppuration in the surgical sites were not found during the whole study period.

Wound healing in the TTT group was faster than in the control and the sham groups, particularly at day 10 and day 14 (Figure 4a). The analysis showed that the wound area percentages were smaller in the TTT group than in the control and the sham groups at these time points (at day 10, TTT vs Control, $p = 0.005$; TTT vs Sham, $p = 0.03$; and at day 14, TTT vs Control, $p < 0.001$; TTT vs Sham, $p = 0.04$) (Figure 4b).

H&E staining displayed that a continuous new epidermis was present at day 8 and day 14, respectively, in the TTT group. By contrast, the newly formed epidermis in both the control and sham groups was irregular and incomplete (Figure 5a). The quantitative analysis demonstrated that the average dermal thickness in the TTT group was greater than in the control and the sham groups (at day 8, TTT vs Control, $p = 0.001$; TTT vs Sham, $p = 0.02$; and at day 14, $p < 0.001$ for all comparisons) (Figure 5b).

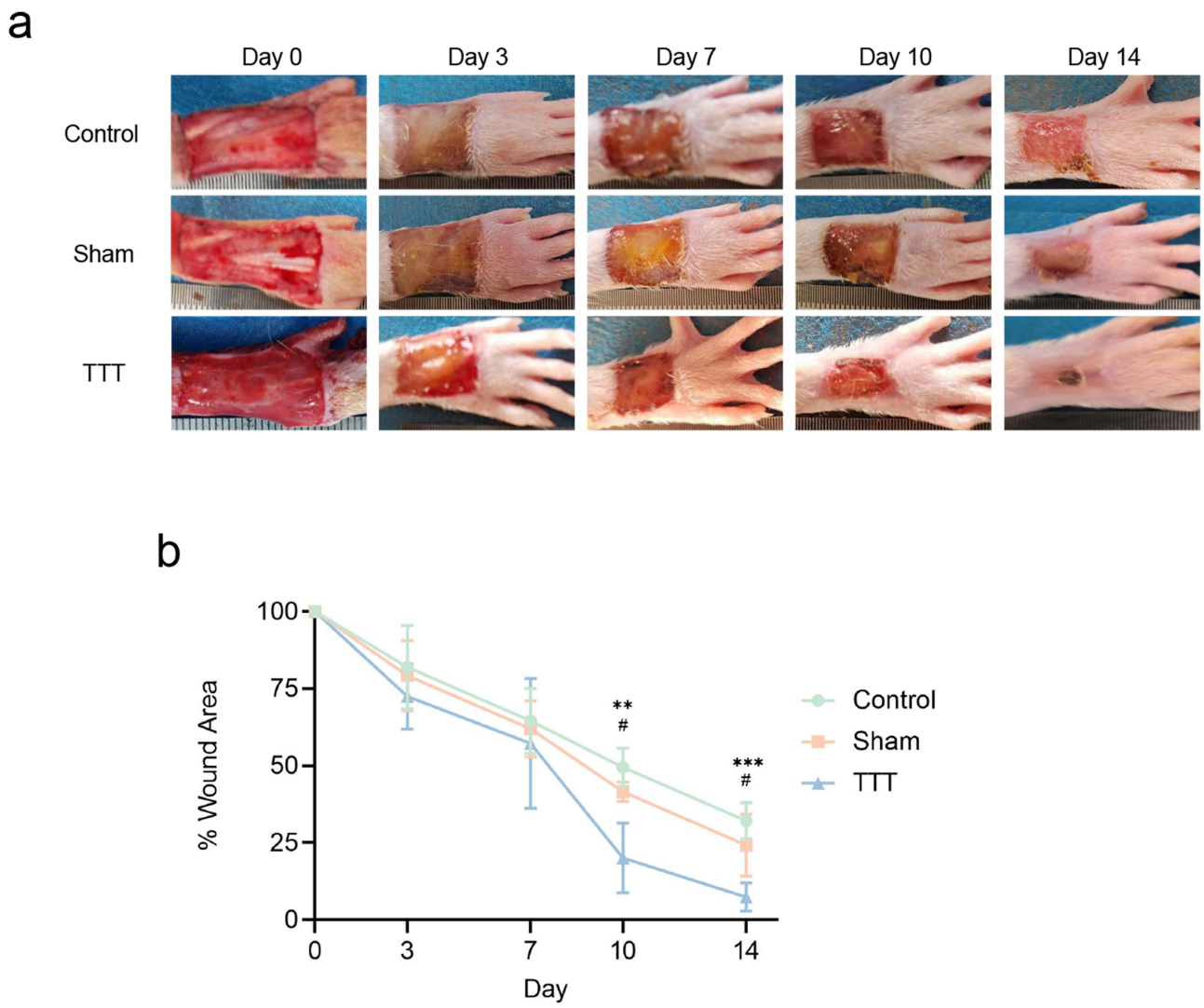

Figure 4 TTT promoted DFU healing. (**a**) Representative images depicting ulcer healing progress for the three groups were captured at days 0, 3, 7, 10, and 14, respectively. (**b**) The wound areas (%) of DFUs in the three groups during observation. **p < 0.01, ***p < 0.001, TTT vs Control; # p < 0.05, TTT vs Sham; Tukey's multiple comparison test was conducted, with n=5 (the number of animals per group).
Abbreviations: TTT, tibial cortex transverse transport; DFU, diabetic foot ulcer.

TTT-Mediated Production and Secretion of Angiogenic Factors

Serum levels of TGF-β1, PDGF-BB, and VEGF were elevated in the TTT group compared to those in the control and the sham groups at day 8 and day 14, respectively (for TGF-β1, at day 8, TTT vs Control, $p < 0.001$ and TTT vs Sham, $p = 0.003$; at day 14, all $p < 0.001$; for PDGF-BB, at day 8, all $p < 0.001$; at day 14, TTT vs Control, $p < 0.001$ and TTT vs Sham, $p = 0.002$; for VEGF, at day 8, TTT vs Control, $p < 0.001$, and TTT vs Sham, $p = 0.007$; at day 14, TTT vs Control, $p = 0.001$ and TTT vs Sham, $p = 0.009$) (Figure 6).

TTT Triggered-Cytokines Enhanced the Proliferation and Migration of EPCs

Flow cytometry analysis revealed that the frequencies of EPCs in both bone marrow and peripheral blood were elevated in the TTT group than those in the control and the sham groups at day 8 and day 14, respectively (at day 8, for bone marrow, TTT vs Control, $p = 0.006$, TTT vs Sham, $p = 0.02$; and for peripheral blood, TTT vs Control, $p = 0.003$, TTT vs Sham, $p = 0.009$; at day 14, for bone marrow, TTT vs Control, $p = 0.002$, TTT vs Sham, $p = 0.01$; and for peripheral blood, TTT vs Control, $p < 0.001$, TTT vs Sham, $p = 0.005$; Figure 7).

https://doi.org/10.2147/JIR.S493505

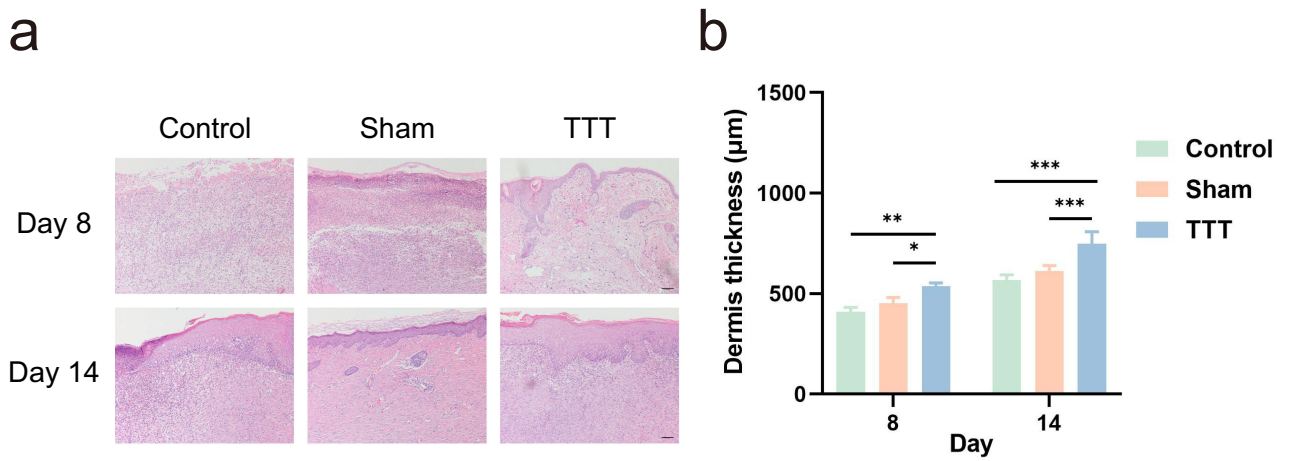

Figure 5 Representative histology images of the three groups at days 8 and 14, respectively. (**a**) Hematoxylin and Eosin staining revealed that the TTT group had less disrupted epidermis than the control and sham groups. Additionally, some hair follicle-like structures (tubular epithelial sheath surrounding the lower part of the hair shaft) were observed in the TTT group. (**b**) After the dermal boundaries were determined using ImageJ software, the dermal thickness was measured. Quantitative analysis revealed that dermal thickness was greater in the TTT group than in the control and sham groups. Scale bar 100 μm. Data are presented as means (standard deviations); *p < 0.05, **p < 0.01, ***p < 0.001. TTT vs Control or Sham was analyzed using Tukey's multiple comparison test.
Abbreviation: TTT, tibial cortex transverse transport.

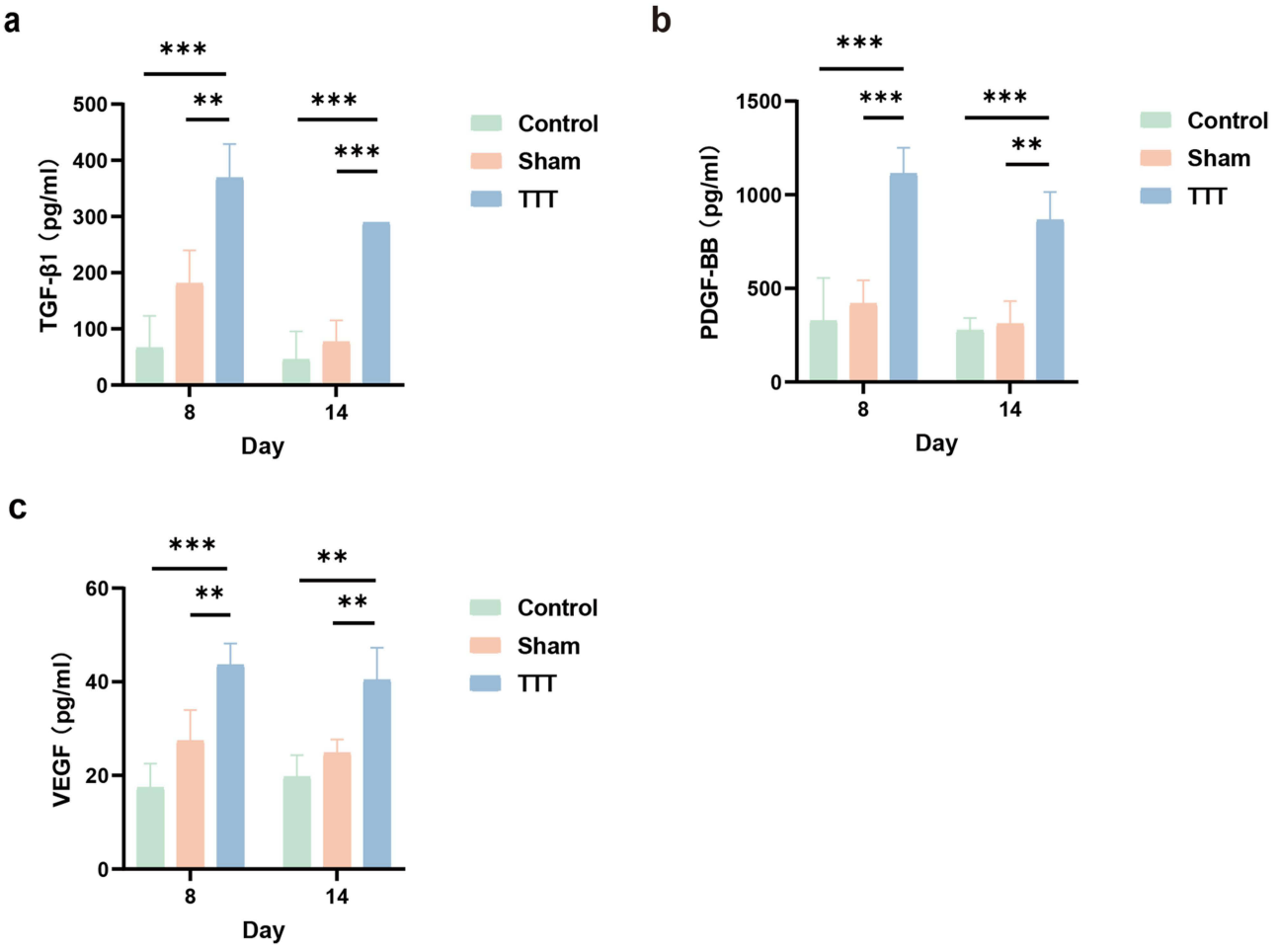

Figure 6 Concentrations of TGF-β1, PDGF-BB, and VEGF in serum after TTT. (**a**) Serum TGF-β1 levels in the TTT group were higher than those in the control and the sham groups at day 8 and 14, respectively. (**b**) The TTT group also showed higher concentrations of serum PDGF-BB than those in the control and the sham groups at the same time points. (**c**) Similarly, VEGF levels in the TTT group were elevated than the control and the sham groups on day 8 and day 14, respectively. Data are presented as means (standard deviations). **p < 0.01, ***p < 0.001, Tukey's multiple comparison test.
Abbreviation: TTT, tibial cortex transverse transport.

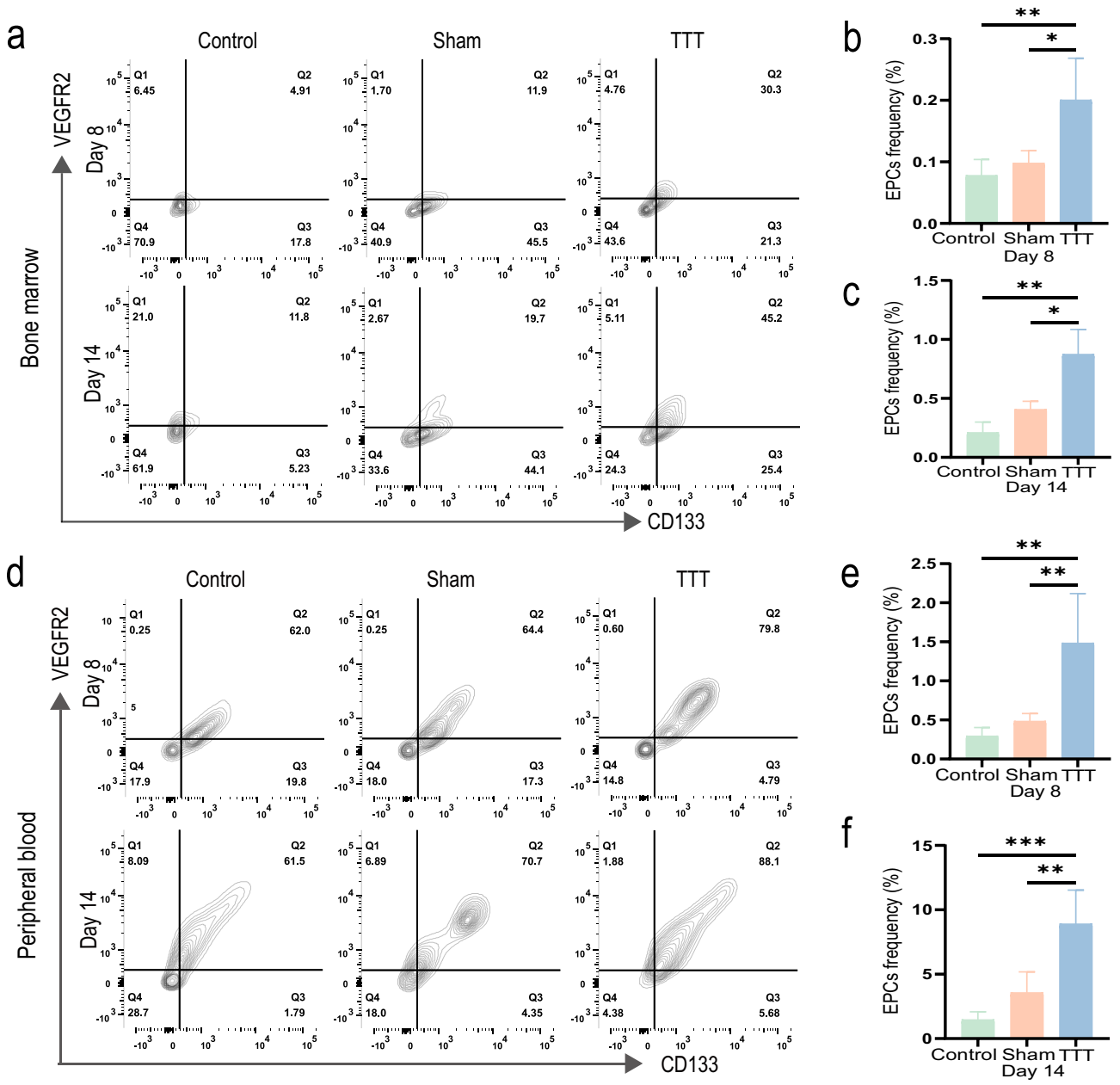

Figure 7 TTT promotes the proliferation and migration of EPCs. The frequency of EPCs was assessed by flow cytometry at day 8 and day 14, respectively. (**a-f**) The frequencies of EPCs in bone marrow and peripheral blood in the TTT group were higher than those in the control and the sham groups at day 8 and day 14, respectively. *p < 0.05, **p < 0.01, ***p < 0.001. Tukey's multiple comparison test. Data are presented as mean ± standard deviation.
Abbreviation: TTT, transverse tibial cortical transport.

Elevated Activity of Ras/Raf/MEK/ERK Pathway After TTT Treatment

The expression of p-ERK1/2 relative to ERK1/2 was higher in the TTT group than those in the control and the sham groups at day 8 and 14, as evaluated by Western Blot (for day 8, TTT vs Control, p = 0.006, and TTT vs Sham, p = 0.007; for day 14, TTT vs Control, p = 0.002, and TTT vs Sham, p = 0.004; Figure 8).

Enhanced Angiogenesis at the Foot Wound After TTT Treatment

The average optical density (AOD) of CD31 and SMA-α in the TTT group was higher than those in the control and the sham groups at day 8 and day 14, respectively, as assessed by immunohistochemistry (for CD31, at day 8, TTT vs Control or TTT vs

https://doi.org/10.2147/JIR.S493505

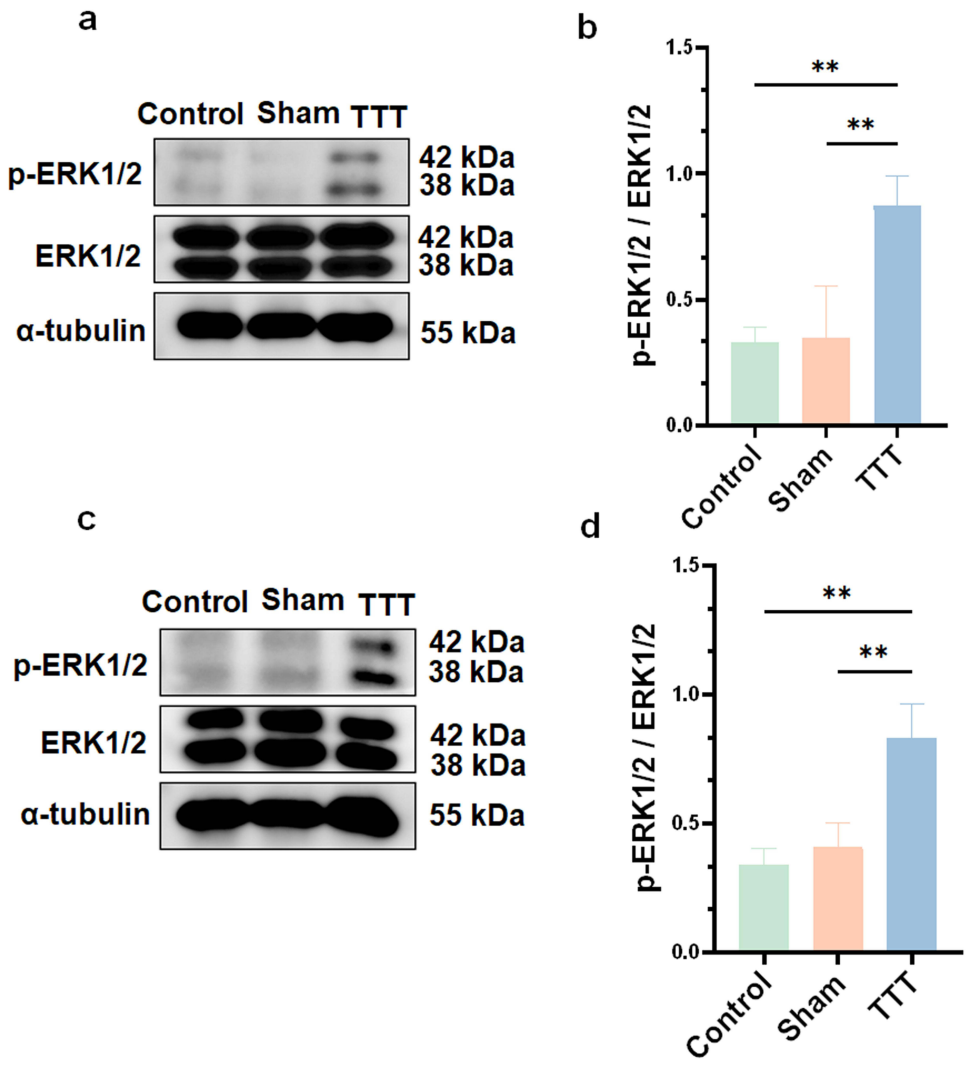

Figure 8 Protein expression of key factors of the Ras/Raf/MEK/ERK signaling pathway. (**a** and **b**) The Western Blot experiments showed that the protein expression levels of p-ERK1/2 relative to ERK1/2 were higher in the TTT group than those in the control and sham groups at day 8. (**c** and **d**) The protein expression levels of p-ERK1/2 relative to ERK1/2 were higher in the TTT group than those in the control and sham groups at day 14. **p < 0.01, Tukey's multiple comparison test. Data are presented as mean ± standard deviation.

Abbreviation: TTT, transverse tibial cortical transport.

Sham, both p = 0.01; at day 14, TTT vs Control, p < 0.001 and TTT vs Sham, p = 0.02; for SMA-α, at day 8, TTT vs Control, p = 0.02, TTT vs Sham, p = 0.04; at day 14, TTT vs Control, p < 0.001, TTT vs Sham, p = 0.002; Figure 9).

The AOD of TGF-β1, PDGF-BB, and VEGF was higher in the TTT group compared to those in the control and the sham groups at day 8 and day 14, respectively (for TGF-β1, at day 8, TTT vs Control, p = 0.02, TTT vs Sham, p = 0.03; at day 14, all p < 0.001; for PDGF-BB, at day 8, TTT vs Control, p = 0.005, and TTT vs Sham, p = 0.04; at day 14, TTT vs Control, p = 0.002, and TTT vs Sham, p = 0.01; for VEGF, at day 8, TTT vs Control, p = 0.008, and TTT vs Sham, p = 0.007; at day 14, TTT vs Control, p = 0.001, and TTT vs Sham, p = 0.01; Figure 10).

The AOD of Ras and Raf in the TTT group was higher than those in the control and the sham groups at day 8 and day 14, respectively (for Ras, at day 8, TTT vs Control, p < 0.001, TTT vs Sham, p = 0.001; at day 14, all p < 0.001; for Raf, at day 8, TTT vs Control, p = 0.006, TTT vs Sham, p = 0.05; at day 14, TTT vs Control, p < 0.001, TTT vs Sham, p = 0.001; Figure 11).

There were no significant differences in the ERK1/2-positive area among the control, the sham, and the TTT groups (Figure 11). However, the p-ERK1/2-positive area was significantly higher in the TTT group compared to the control and the sham groups (at day 8, all p < 0.001, at day 14, TTT vs Control, p < 0.001, TTT vs Sham, p = 0.01; Figure 11).

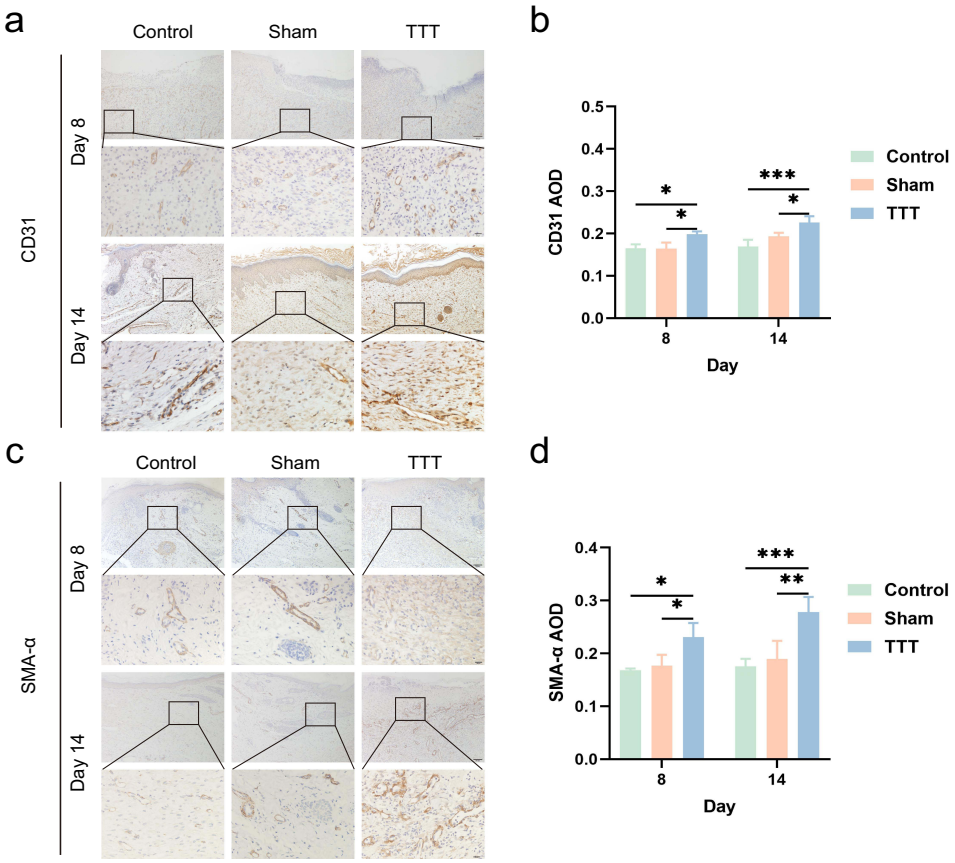

Figure 9 Elevated expression of CD31 and SMA-α in diabetic wounds after TTT treatment. (**a**) Representative immunohistochemical images of CD31 expression in the groups at day 8 and day 14, respectively. (**b**) Quantitative analysis revealed that the AOD of CD31 was higher in the TTT group than in the control and sham groups. (**c**) Representative immunohistochemical images of SMA-α expression in the three groups at day 8 and day 14, respectively. (**d**) Quantitative analysis revealed that the AOD of SMA-α in the TTT group was elevated than the control and the sham groups. Data are expressed as mean (standard deviation), *p < 0.05, **p < 0.01, ***p < 0.001. TTT vs Control or Sham, Tukey's multiple comparison test. Day 8 scale bar 100 μm, magnification 100 times; day 14 scale bar 20 μm, magnification 400 times.
Abbreviations: TTT, transverse tibial cortical transport; AOD, average optical density.

Discussion

In this study, we investigated the healing process, changes in angiogenesis at the foot wound, and the activity of EPCs and the Ras/Raf/MEK/ERK pathway in DFUs after TTT, an ideal model of continuous microinjuries. We found that the production of multiple angiogenic factors and the activity of EPCs and the Ras/Raf/MEK/ERK pathway were elevated after TTT; correspondingly, there was enhanced angiogenesis at the foot wound and DFU healing. These findings suggest that remote continuous microinjuries (ie, TTT) can trigger the production of multiple angiogenic factors that in turn enhance the proliferation and migration of EPCs to the target tissues via peripheral circulation via the Ras/Raf/MEK/ERK pathway, ultimately contributing to tissue repair.

Injury can trigger localized tissue repair or regeneration.[1,2] However, although small injuries can be healed with the body's adjustment, large-scale damages or non-healing pathological defects usually need special regenerative treatments. Distraction osteogenesis, or bone transport, was originally developed by Ilizarov[3,4] and consists of continuous micro-injuries. Given that distraction osteogenesis was accompanied by angiogenesis, we and other groups applied TTT to patients with recalcitrant DFUs and attained obvious clinical effects, and we found increased neovascularization and perfusion at the foot after TTT treatment.[5,22,23] Accordingly, here we proposed the theory that controlled remote continuous microinjuries can be used to stimulate the intrinsic repair ability of the body, which enhances the repair of the localized tissue, and, more importantly, the target tissues. These injuries should have several characteristics. First, they should be microinjuries so they can trigger the production of pro-regenerative cytokines while being minimally invasive and avoiding severe tissue damage which may be difficult to heal themselves or heal with scar formation.

https://doi.org/10.2147/JIR.S493505

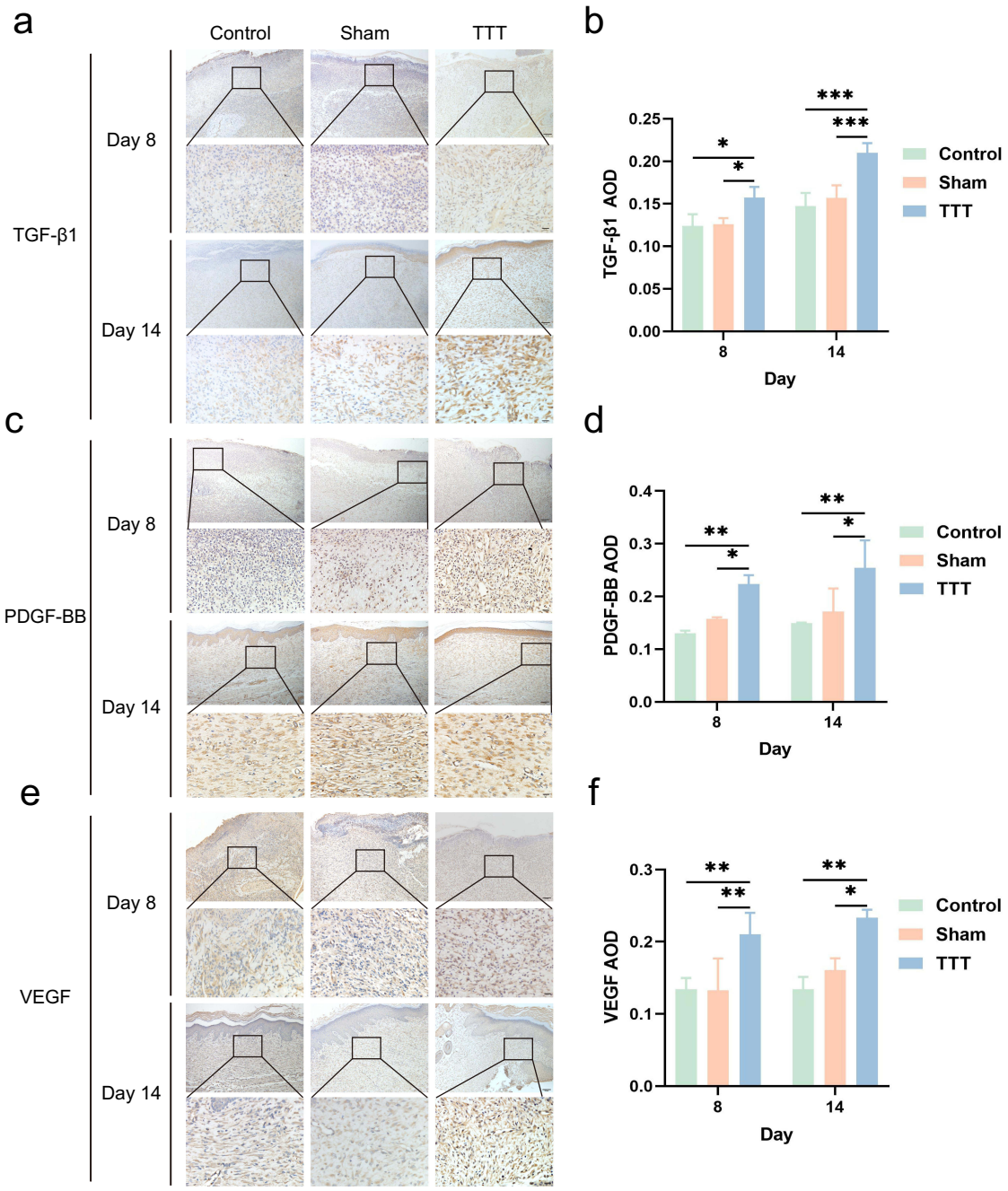

Figure 10 Elevated expression of TGF-β1, PDGF-BB, and VEGF in diabetic wounds after TTT. (**a**) Representative immunohistochemical images of TGF-β1 expression in the three groups at day 8 and day 14, respectively. (**b**) Analysis revealed that the AOD of TGF-β1 in the TTT group was higher than in the control and the sham groups. (**c**) Representative immunohistochemical images of PDGF-BB expression in the three groups at day 8 and day 14, respectively. (**d**) Analysis displayed that the AOD of PDGF-BB in the TTT group was higher than in the control and sham groups. (**e**) Representative immunohistochemical images of VEGF expression in the three groups of rats at day 8 and day 14, respectively. (**f**) Analysis showed that the AOD of VEGF in the TTT group was higher than in the control and sham groups. Data are expressed as mean (standard deviation), *$p < 0.05$, **$p < 0.01$, ***$p < 0.001$. TTT vs Control or Sham, Tukey's multiple comparison test. Day 8 scale bar 100 μm, magnification 100 times; day 14 scale bar 20 μm, magnification 400 times.
Abbreviations: TTT, transverse tibial cortical transport; AOD, average optical density.

Second, the microinjuries should be continuous so they can stimulate persistent cytokine release which can match the healing process of the target tissues. This also indicates that the microinjuries should be controllable or suitable for self-administration by patients. Third, the microinjuries can be distant to the target damaged tissues so they will not cause further injuries to the target tissues. The essence of remote microinjuries is just to mimic the body's sophisticated functions and strategies for intrinsic repair. To further confirm this theory and explore the underlying mechanism, we

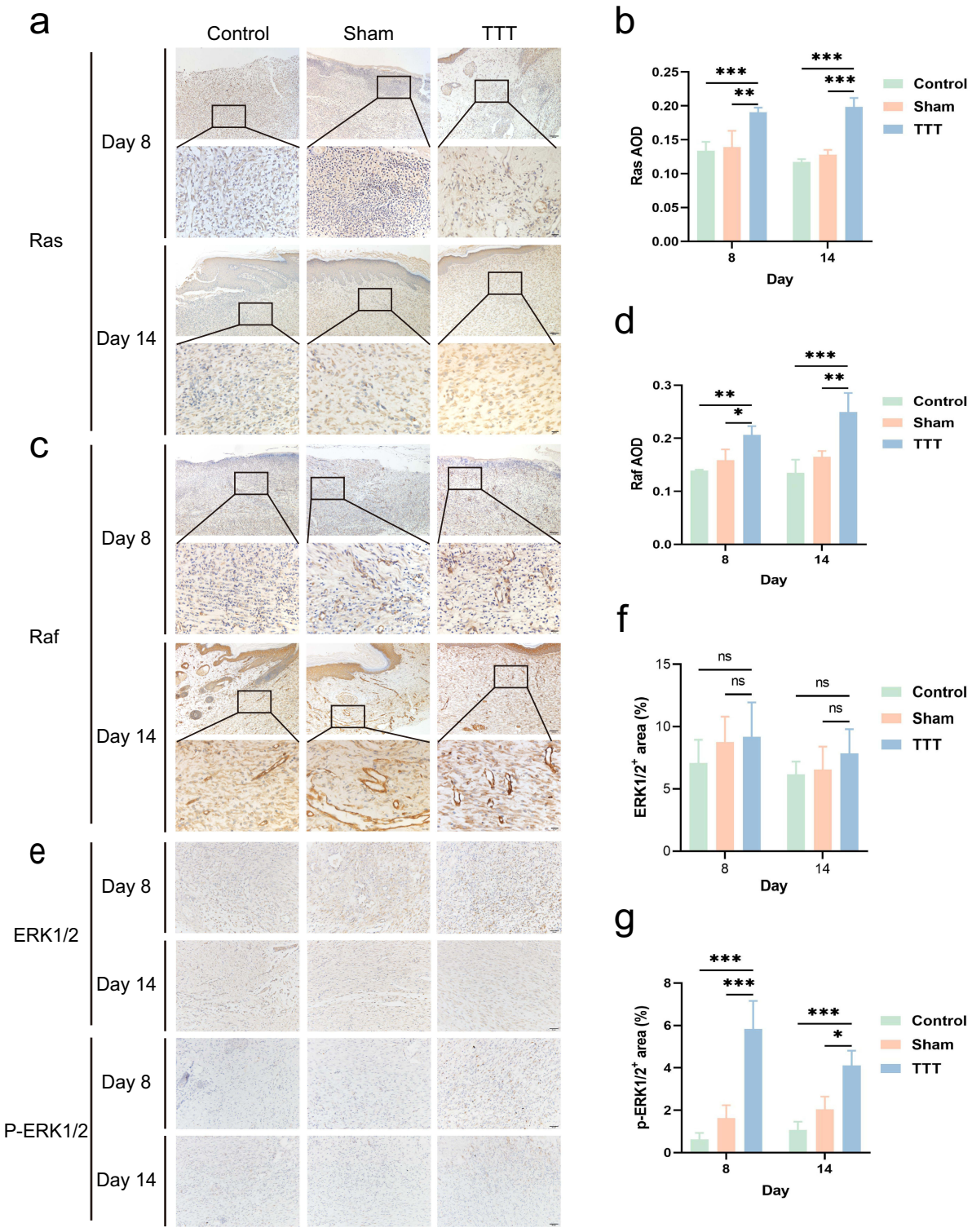

Figure 11 Elevated expression of Ras, Raf, and p-ERK1/2 in diabetic wounds after TTT. (**a**) Representative immunohistochemical images of Ras expression at day 8 and 14, respectively. Day 8 scale bar 100 μm, magnification 100 times; day 14 scale bar 20 μm, magnification 400 times. (**b**) Analysis revealed that the AOD of Ras in the TTT group was higher than in the control and sham groups. Day 8 scale bar 100 μm, magnification 100 times; day 14 scale bar 20 μm, magnification 400 times. (**c**) Representative immunohistochemical images of Raf expression at day 8 and day 14, respectively. (**d**) Analysis showed that the AOD of Raf was higher in the TTT group than in the other groups. (**e**) Representative immunohistochemical images of ERK1/2 and p-ERK1/2 expression in the three groups at day 8 and day 14, respectively. Day 8 and day 14 scale bar 50 μm, magnification 200 times. (**f**) Analysis displayed that there was no difference in the ERK1/2$^+$ area among the three groups. (**g**) Analysis revealed that the p-ERK1/2$^+$ area was higher in the TTT group than in the control and sham groups. Data are expressed as mean (standard deviation), *p < 0.05, **p < 0.01, ***p < 0.001. TTT vs Control or Sham, Tukey's multiple comparison test.

Abbreviations: TTT, transverse tibial cortical transport; AOD, average optical density.

https://doi.org/10.2147/JIR.S493505

developed a rat model of DFUs treated using TTT, an ideal model of remote continuous microinjuries. Consistently, we observed enhanced neovascularization in the hindlimb, along with accelerated DFU healing.[34] However, the exact mechanism of this theory is still unclear.

In our previous clinical studies on the management of recalcitrant DFUs using TTT, evaluation of neovascularization using computed tomography angiography, and assessment of blood flow and blood volume using computed tomography perfusion were not performed in the control group.[22,23] Thus, a causal relationship between TTT and DFU healing was not established. Furthermore, tibial fractures have been associated with increased blood flow in the foot muscle and skin;[44] but our study did not include a cohort undergoing tibial corticotomy (tibial fracture) alone (without distraction) because we were concerned that this treatment would be ineffective. Thus, we cannot rule out the possibility that tibial corticotomy independently improves foot perfusion and wound healing in severe DFUs. In this study, we included a sham surgery group (corticotomy without cortex transport) for comparison with both the TTT and control groups. Our results showed that although the peripheral blood levels of TGF-β1, PDGF-BB, and VEGF were elevated in the sham group compared to the control group, these differences were not statistically significant. This finding is consistent with the results of wound healing, immunohistochemistry, Western Blot, and flow cytometry, suggesting that the effect of corticotomy alone may be not enough, if any, for the treatment of severe DFUs. Moreover, our results demonstrate enhanced angiogenesis and ulcer healing in the TTT group than the sham group, supporting that the beneficial effects of TTT on DFU healing are largely attributed to transverse cortex distraction.

One important finding of the present study was the activation of EPCs following TTT surgery. EPCs are essential for the repair of damaged blood vessels and the formation of new vessels in ischemic tissues.[25,45,46] In individuals with DFUs, the number and function of EPCs are reduced, resulting in a diminished capacity to promote angiogenesis.[47] Previous studies have emphasized that the impaired function and decreased number of EPCs in diabetic patients contribute to the chronicity and severity of diabetic ulcers.[47] In the current study, we found increased EPC frequency in both bone marrow and peripheral blood, as evaluated by flow cytometry. Thus, the activation of EPCs is one of the main mechanisms of the TTT treatment for DFU healing. Nevertheless, how the EPCs sense the TTT stimuli and translate them into biological effects needs further studies in the future.

Previous studies have tried to explore the role of EPCs in DFUs treated using TTT.[28,48] However, there is some controversy over the use of surface markers to identify EPCs using flow cytometry. One study defined EPCs in peripheral circulation in a rabbit model of TTT using two markers, CD34 and CD133.[48] Another study identified EPCs in peripheral blood in a rat model of TTT using another two markers, VEGFR2 and Tie-2.[28] The results of the two studies are inconsistent.[28,48] The possible reasons for such a discrepancy are that the EPC markers and TTT protocols used were different between the two studies. In this study, we employed more comprehensive markers, CD34, CD133, and VEGFR2, for EPC detection.[49] We found increased frequencies of EPCs in the peripheral blood in the TTT group, in line with the previous studies.[28,48] This indicates that TTT promotes EPC migration through the secretion of cytokines such as TGF-β1, PDGF-BB, and VEGF. In addition, a prior study detected the proportion of EPCs in peripheral blood at only one-time point (at day 10 postoperatively),[50] thus it is impossible to determine the longitudinal changes of EPC activity. In contrast, in this study, evaluation of the EPC frequencies at two-time points (at day 8 and day 14 post-operatively, respectively) allows us to determine that the continuous microfractures in TTT have a persistent effect on EPC migration and proliferation.

EPCs primarily reside in the bone marrow and may proliferate and migrate in response to stimuli.[25] Although previous studies did detect the changes in EPCs in the peripheral blood after TTT, they did not investigate the effect of TTT on bone marrow EPCs.[28,48] In this study, we evaluated the changes in the number of EPCs in the bone marrow after TTT and found an increased frequency of EPCs. This suggests a direct proliferative effect of TTT on EPCs. Moreover, we found markedly higher frequencies of EPCs in the peripheral blood than in bone marrow, indicating that EPCs further proliferate after entering peripheral circulation mediated by TGF-β1, PDGF-BB, and VEGF.[28,48] Together, our findings demonstrated that TTT not only promoted the migration of EPCs to the ischemic sites but also their initial proliferation in the bone marrow.

The activation of EPCs can be regulated by different pathways.[48,50] Previous studies have investigated the role of several signaling pathways, such as SDF-1/CXCR4 and the store-operated calcium entry (SOCE) pathways, in angiogenesis after TTT treatment.[48,51] Another crucial pathway for angiogenesis is the Ras/Raf/MEK/ERK pathway.[29,52] This

pathway is widely recognized for its role in cell proliferation, differentiation, and survival, with its activation being essential for effective angiogenesis.[52,53] Previous studies demonstrated that the Ras/Raf/MEK/ERK pathway is activated by the TGF-β1, PDGF-BB, and VEGF.[29,52,54] However, no studies have reported the role of the Ras/Raf/MEK/ERK pathway in angiogenesis and wound healing in the treatment of DFU using TTT. In this study, we detected increased activity of the Ras/Raf/MEK/ERK pathway, in parallel with elevated production and secretion of TGF-β1, PDGF-BB, and VEGF, activity of EPCs, angiogenesis at the foot wound, and enhanced wound healing. Thus, our results may generate a model of "Enhanced angiogenesis and activation of EPCs by TTT-triggered cytokines contributing to DFU healing" for the mechanism of DFU treatment using TTT (Figure 12).

This study has several limitations. First, while our rat model reflects the severity and ischemic aspects of DFUs, including wound size, depth, and arterial ligation, it does not encompass other crucial disease components such as sustained inflammation, malnutrition, infections, neuropathy, aging, and primary healing mechanism (through contraction in rodents vs re-epithelialization in humans).[55] Second, our choice of not using mice, a more common species for DFU studies, was based on practical considerations. While mice offer species-specific reagents and genetic modification potential, their small tibial diameter complicates the surgical procedures, like creating a partial tibial corticotomy and

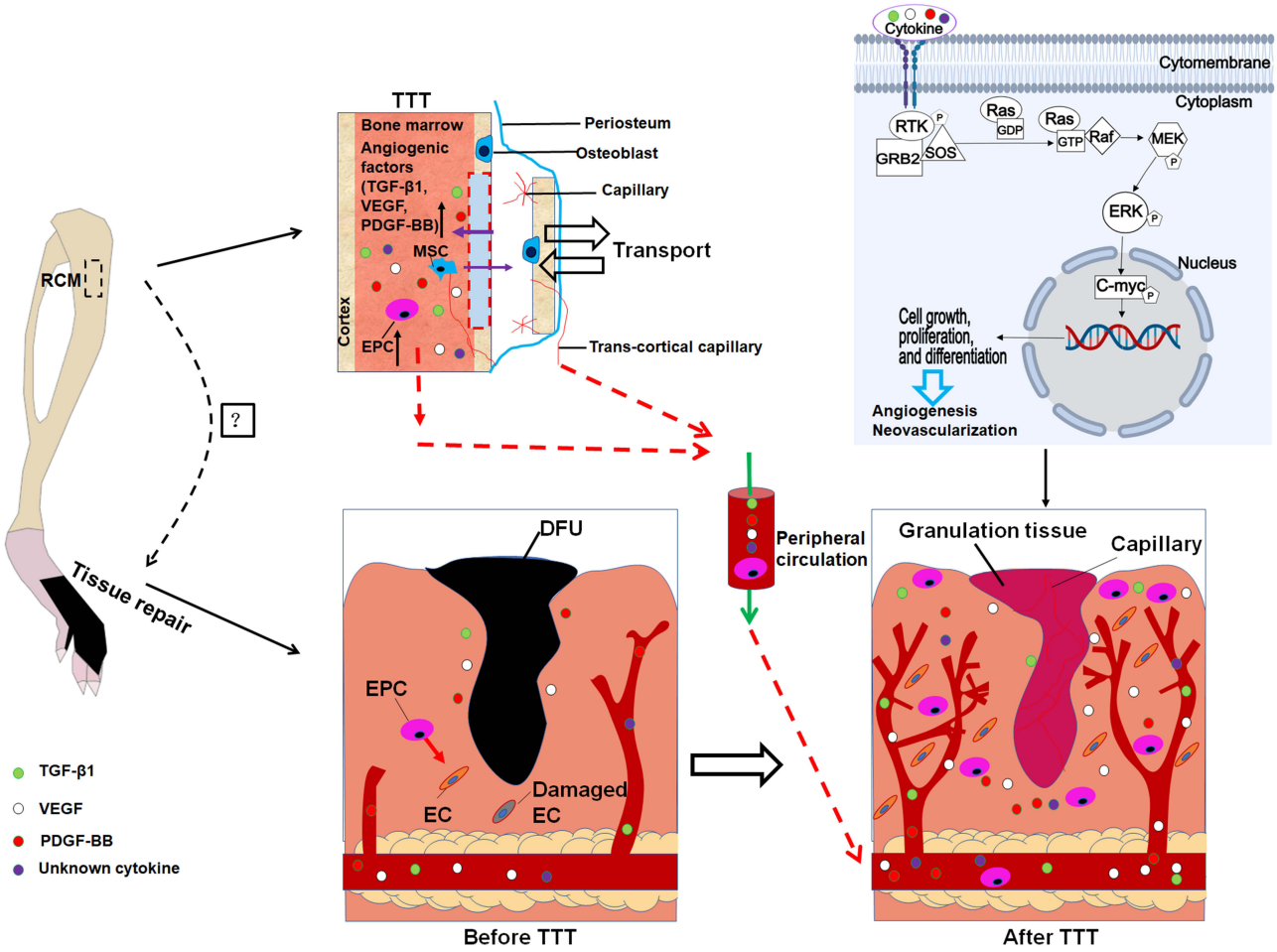

Figure 12 Model of continuous microinjury-triggered cytokines activating EPCs to treat DFU. The question mark (middle left) represents the research question of the current study – how continuous microinjuries (ie, tibial transport) contribute to remote tissue repair (ie, foot wound healing). The model proposed based on the results of the current study is that TTT mediates the production of cytokines (such as TGF-β1, PDGF-BB, and VEGF) which in turn activate EPCs via the Ras/Raf/MEK/ERK pathway, leading to EPC proliferation in the bone marrow and migration into the peripheral blood. EPCs further travel to the foot wound through the peripheral circulation, contributing to different effects including angiogenesis, granulation tissue formation, and ultimately wound healing. In addition, some of the secreted cytokines travel directly to the foot wound and enhance wound healing. The circles of different colors indicate different cytokines triggered by TTT.

Abbreviations: BM-MSC, bone marrow mesenchymal stem cell; DFU, diabetic foot ulcer; TTT, tibial cortex transverse transport; EPCs, endothelial progenitor cells; EC, endothelial cell.

https://doi.org/10.2147/JIR.S493505

applying an external distractor for transverse distraction. On the other hand, using rats allowed us to create larger and deeper ulcers, more closely mimicking the DFUs encountered frequently in clinical settings. Third, the STZ-induced diabetes model used primarily represents acute diabetes and does not fully mimic the chronic neurological and endothelial pathologies observed in human diabetes; and the wound model applied was an acute rather than a chronic wound model. However, the STZ model is widely used in preclinical research because it reliably induces hyperglycemia and facilitates the study of diabetes-related complications, including delayed wound healing.[35] Furthermore, this model is cost-effective. While chronic models may offer more similarities to human pathology, they come with challenges such as extended study durations and higher costs. Moreover, studies reported that the acute wound models can provide useful information on wound healing and are cost-effective.[34,55,56] Despite this, a model of chronic diabetes with chronic wound that more closely resembles DFUs should be used in future studies. Fourth, hair follicle-like structures were found in the TTT group while hardly observed in the control or the sham groups as evaluated by histology. However, we did not perform specific staining (eg, immunohistochemistry) to confirm these structures were hair follicles. Thus, we could not conclude that TTT enhances hair follicle regeneration at the foot wound. Further studies are needed to examine the effect of TTT on foot tissue regeneration. Fifth, our study did not incorporate inhibitors or agonists to manipulate the Ras/Raf/MEK/ERK pathway. Therefore, we did not directly test the causal effects of specific signaling pathways, and thus the role of this pathway in the treatment of TTT for DFUs warrants further corroboration. Last, although we proposed the theory of remote continuous microinjury-induced repair and TTT used in this study is just an ideal model of continuous microinjuries, more studies are still needed to validate this theory. Future research on remote continuous microinjury-induced repair needs to incorporate long-term follow-up (eg, 6–12 weeks) to evaluate its long-term effects and assess the potential side effects or complications.

In conclusion, our results showed that TTT, a technique involving continuous microinjuries, facilitates angiogenesis at the foot and ultimately DFU healing. The underlying mechanism is that TTT triggered the production of multiple cytokines which traveled to the foot wound and enhanced wound healing. Moreover, the cytokines promoted the proliferation and migration of EPCs to the foot wound via activation of the Ras/Raf/MEK/ERK pathway, further contributing to wound healing. The findings suggest that remote continuous microinjuries can serve as an approach for target tissue repair. Our findings warrant future studies with larger and more diverse human populations and extended follow-up periods to confirm the results and assess long-term effects to validate the theory of remote continuous microinjury-induced repair.

Data Sharing Statement

The data are provided in the manuscript or figures.

Ethics Approval

Our animal study adhered to the guidelines set forth by the National Institutes of Health and received approval from The First Affiliated Hospital of Guangxi Medical University Animal Ethics Committee (Reference Number: 2022-D170-01).

Author Contributions

All authors made a significant contribution to the work reported, whether that is in the conception, study design, execution, acquisition of data, analysis, and interpretation, or in all these areas; took part in drafting, revising, or critically reviewing the article; gave final approval of the version to be published; have agreed on the journal to which the article has been submitted; and agree to be accountable for all aspects of the work.

Funding

This study was supported by grants from National Natural Science Foundation of China (82060406, 82360429, 82260448), Joint Project on Regional High-incidence Diseases Research of Natural Science Foundation of Guangxi (2022JJA141126), Advanced Innovation Teams and Xinghu Scholars Program of Guangxi Medical University, China Postdoctoral Science Foundation (2019M650235), Key R&D Project of Qingxiu District, Nanning, Guangxi (2021003), Clinical research climbing plan of the First Affiliated Hospital of Guangxi Medical University (YYZS2020010).

Disclosure

None of the authors have any conflicts of interest to declare for this work.

References

1. Eming SA, Martin P, Tomic-Canic M. Wound repair and regeneration: mechanisms, signaling, and translation. *Sci Transl Med*. 2014;6(265):265sr6. doi:10.1126/scitranslmed.3009337
2. Long L, Ji D, Hu C, Yang L, Tang S, Wang Y. Microneedles for in situ tissue regeneration. *Mater Today Bio*. 2023;19:100579. doi:10.1016/j.mtbio.2023.100579
3. Ilizarov GA. The tension-stress effect on the genesis and growth of tissues. Part I. The influence of stability of fixation and soft-tissue preservation. *Clin Orthop*. 1989;238:249–281. doi:10.1097/00003086-198901000-00038
4. Ilizarov GA. The tension-stress effect on the genesis and growth of tissues: part II. The influence of the rate and frequency of distraction. *Clin Orthop*. 1989;239:263–285. doi:10.1097/00003086-198902000-00029
5. Liu G, Li S, Kuang X, et al. The emerging role of tibial cortex transverse transport in the treatment of chronic limb ischemic diseases. *J Orthop Transl*. 2020;25:17–24. doi:10.1016/j.jot.2020.10.001
6. Troulis MJ, Padwa B, Kaban LB. Distraction osteogenesis: past, present, and future. *Facial Plast Surg FPS*. 1998;14(3):205–215. doi:10.1055/s-2008-1064346
7. Ilizarov GA, Ledyaev VI. The replacement of long tubular bone defects by lengthening distraction osteotomy of one of the fragments. *Clin Orthop*. 1992;280:7–10. doi:10.1097/00003086-199207000-00002
8. Ilizarov GA. Clinical application of the tension-stress effect for limb lengthening. *Clin Orthop*. 1990;250:8–26. doi:10.1097/00003086-199001000-00003
9. Minematsu K, Tsuchiya H, Taki J, Tomita K. Blood flow measurement during distraction osteogenesis. *Clin Orthop*. 1998;347:229–235. doi:10.1097/00003086-199802000-00028
10. Gubin AV, Borzunov DY, Marchenkova LO, Malkova TA, Smirnova IL. Contribution of G.A. Ilizarov to bone reconstruction: historical achievements and state of the art. *Strategies Trauma Limb Reconstr*. 2016;11(3):145–152. doi:10.1007/s11751-016-0261-7
11. Kuo KN, Qureshi A, Bush-Joseph CA, Templeton A. Ilizarov distraction histogenesis to reconstruct massive posttraumatic osteoarticular defects: a case report. *J Bone Joint Surg Am*. 2003;85(6):1125–1128. doi:10.2106/00004623-200306000-00025
12. Aston JW, Williams SA, Allard RN, Sawamura S, Carollo JJ. A new canine cruciate ligament formed through distraction histogenesis. Report of a pilot study. *Clin Orthop*. 1992;280:30–36. doi:10.1097/00003086-199207000-00006
13. Matsuyama J, Ohnishi I, Kageyama T, Oshida H, Suwabe T, Nakamura K. Osteogenesis and angiogenesis in regenerating bone during transverse distraction: quantitative evaluation using a canine model. *Clin Orthop*. 2005;433:243–250. doi:10.1097/01.blo.0000150562.24256.a4
14. Ohashi S, Ohnishi I, Kageyama T, Imai K, Nakamura K. Distraction osteogenesis promotes angiogenesis in the surrounding muscles. *Clin Orthop*. 2007;454:223–229. doi:10.1097/01.blo.0000238795.82466.74
15. Sun H, Saeedi P, Karuranga S, et al. IDF Diabetes Atlas: global, regional and country-level diabetes prevalence estimates for 2021 and projections for 2045. *Diabet Res Clin Pract*. 2022;183:109119. doi:10.1016/j.diabres.2021.109119
16. Senneville É, Albalawi Z, van Asten SA, et al. IWGDF/IDSA guidelines on the diagnosis and treatment of diabetes-related foot infections (IWGDF/IDSA 2023). *Clin Infect Dis off Publ Infect Dis Soc Am*. 2023:ciad527. doi:10.1093/cid/ciad527
17. Boulton AJM, Vileikyte L, Ragnarson-Tennvall G, Apelqvist J. The global burden of diabetic foot disease. *Lancet Lond Engl*. 2005;366(9498):1719–1724. doi:10.1016/S0140-6736(05)67698-2
18. McDermott K, Fang M, Boulton AJM, Selvin E, Hicks CW. Etiology, epidemiology, and disparities in the burden of diabetic foot ulcers. *Diabetes Care*. 2023;46(1):209–221. doi:10.2337/dci22-0043
19. Edmonds M, Manu C, Vas P. The current burden of diabetic foot disease. *J Clin Orthop Trauma*. 2021;17:88–93. doi:10.1016/j.jcot.2021.01.017
20. Chuter V, Schaper N, Mills J, et al. Effectiveness of revascularisation for the ulcerated foot in patients with diabetes and peripheral artery disease: a systematic review. *Diabetes Metab Res Rev*. 2024;40(3):e3700. doi:10.1002/dmrr.3700
21. Leibson CL, Ransom JE, Olson W, Zimmerman BR, O'fallon WM, Palumbo PJ. Peripheral arterial disease, diabetes, and mortality. *Diabetes Care*. 2004;27(12):2843–2849. doi:10.2337/diacare.27.12.2843
22. Chen Y, Ding X, Zhu Y, et al. Effect of tibial cortex transverse transport in patients with recalcitrant diabetic foot ulcers: a prospective multicenter cohort study. *J Orthop Transl*. 2022;36:194–204.
23. Chen Y, Kuang X, Zhou J, et al. Proximal tibial cortex transverse distraction facilitating healing and limb salvage in severe and recalcitrant diabetic foot ulcers. *Clin Orthop*. 2020;478(4):836–851.
24. Obi S, Yamamoto K, Ando J. Effects of shear stress on endothelial progenitor cells. *J Biomed Nanotechnol*. 2014;10(10):2586–2597. doi:10.1166/jbn.2014.2014
25. Asahara T, Murohara T, Sullivan A, et al. Isolation of putative progenitor endothelial cells for angiogenesis. *Science*. 1997;275(5302):964–967. doi:10.1126/science.275.5302.964
26. Wils J, Favre J, Bellien J. Modulating putative endothelial progenitor cells for the treatment of endothelial dysfunction and cardiovascular complications in diabetes. *Pharmacol Ther*. 2017;170:98–115. doi:10.1016/j.pharmthera.2016.10.014
27. Fadini GP, Losordo D, Dimmeler S. Critical reevaluation of endothelial progenitor cell phenotypes for therapeutic and diagnostic use. *Circ Res*. 2012;110(4):624–637. doi:10.1161/CIRCRESAHA.111.243386
28. Tian W, Feng B, Zhang L, et al. Tibial transverse transport induces mobilization of endothelial progenitor cells to accelerate angiogenesis and ulcer wound healing through the VEGFA/CXCL12 pathway. *Biochem Biophys Res Commun*. 2024;709:149853. doi:10.1016/j.bbrc.2024.149853
29. Song YY, Liang D, Liu DK, Lin L, Zhang L, Yang WQ. The role of the ERK signaling pathway in promoting angiogenesis for treating ischemic diseases. *Front Cell Dev Biol*. 2023;11:1164166. doi:10.3389/fcell.2023.1164166
30. Liao ZH, Zhu HQ, Chen YY, et al. The epigallocatechin gallate derivative Y6 inhibits human hepatocellular carcinoma by inhibiting angiogenesis in MAPK/ERK1/2 and PI3K/AKT/ HIF-1α/VEGF dependent pathways. *J Ethnopharmacol*. 2020;259:112852. doi:10.1016/j.jep.2020.112852

31. Frémin C, Saba-El-Leil MK, Lévesque K, Ang SL, Meloche S. Functional redundancy of ERK1 and ERK2 MAP kinases during development. *Cell Rep*. 2015;12(6):913–921. doi:10.1016/j.celrep.2015.07.011
32. Chappell WH, Steelman LS, Long JM, et al. Ras/Raf/MEK/ERK and PI3K/PTEN/Akt/mTOR inhibitors: rationale and importance to inhibiting these pathways in human health. *Oncotarget*. 2011;2(3):135–164. doi:10.18632/oncotarget.240
33. Phimnuan P, Dirand Z, Tissot M, et al. Beneficial effects of a blended fibroin/aloe gel extract film on the biomolecular mechanism(s) via the MAPK/ERK pathway relating to diabetic wound healing. *ACS Omega*. 2023;8(7):6813–6824. doi:10.1021/acsomega.2c07507
34. Liu J, Huang X, Su H, et al. Tibial cortex transverse transport facilitates severe diabetic foot wound healing via HIF-1α-induced angiogenesis. *J Inflamm Res*. 2024;17:2681–2696. doi:10.2147/JIR.S456590
35. Furman BL. Streptozotocin-induced diabetic models in mice and rats. *Curr Protoc Pharmacol*. 2015;70(1). doi:10.1002/0471141755.ph0547s70
36. Guo SC, Tao SC, Yin WJ, Qi X, Yuan T, Zhang CQ. Exosomes derived from platelet-rich plasma promote the re-epithelization of chronic cutaneous wounds via activation of YAP in a diabetic rat model. *Theranostics*. 2017;7(1):81–96. doi:10.7150/thno.16803
37. Całkosiński I, Gostomska-Pampuch K, Majda J, et al. The influence of α-tocopherol on serum biochemical markers during experimentally induced pleuritis in rats exposed to dioxin. *Inflammation*. 2017;40(3):913–926. doi:10.1007/s10753-017-0536-2
38. Schneider CA, Rasband WS, Eliceiri KW. NIH Image to ImageJ: 25 years of image analysis. *Nat Methods*. 2012;9(7):671–675. doi:10.1038/nmeth.2089
39. Chen Y, Huang YC, Yan CH, et al. Abnormal subchondral bone remodeling and its association with articular cartilage degradation in knees of type 2 diabetes patients. *Bone Res*. 2017;5:17034. doi:10.1038/boneres.2017.34
40. Chen Y, Hu Y, Yu YE, et al. Subchondral trabecular rod loss and plate thickening in the development of osteoarthritis. *J Bone Miner Res off J Am Soc Bone Miner Res*. 2018;33(2):316–327. doi:10.1002/jbmr.3313
41. Khorasani H, Zheng Z, Nguyen C, et al. A quantitative approach to scar analysis. *Am J Pathol*. 2011;178(2):621–628. doi:10.1016/j.ajpath.2010.10.019
42. Chen Y, Wang T, Guan M, et al. Bone turnover and articular cartilage differences localized to subchondral cysts in knees with advanced osteoarthritis. *Osteoarthritis Cartilage*. 2015;23(12):2174–2183. doi:10.1016/j.joca.2015.07.012
43. Shapiro SS, Wilk MB. An analysis of variance test for normality (complete samples)†. *Biometrika*. 1965;52(3–4):591–611. doi:10.1093/biomet/52.3-4.591
44. Kellerová E, Delius W, Olerud S, Ström G. Changes in the muscle and skin blood flow following lower leg fracture in man. *Acta Orthop Scand*. 1970;41(3):249–260. doi:10.3109/17453677008991512
45. Rakkar K, Othman O, Sprigg N, Bath P, Bayraktutan U. Endothelial progenitor cells, potential biomarkers for diagnosis and prognosis of ischemic stroke: protocol for an observational case-control study. *Neural Regen Res*. 2020;15(7):1300–1307. doi:10.4103/1673-5374.269028
46. Tepper OM, Capla JM, Galiano RD, et al. Adult vasculogenesis occurs through in situ recruitment, proliferation, and tubulization of circulating bone marrow-derived cells. *Blood*. 2005;105(3):1068–1077. doi:10.1182/blood-2004-03-1051
47. Pyšná A, Bém R, Němcová A, et al. Endothelial progenitor cells biology in diabetes mellitus and peripheral arterial disease and their therapeutic potential. *Stem Cell Rev Rep*. 2019;15(2):157–165. doi:10.1007/s12015-018-9863-4
48. Ou S, Wu X, Yang Y, et al. Tibial cortex transverse transport potentiates diabetic wound healing via activation of SDF-1/CXCR4 signaling. *PeerJ*. 2023;11:e15894. doi:10.7717/peerj.15894
49. Massa M, Rosti V, Ramajoli I, et al. Circulating CD34+, CD133+, and vascular endothelial growth factor receptor 2-positive endothelial progenitor cells in myelofibrosis with myeloid metaplasia. *J Clin Oncol off J Am Soc Clin Oncol*. 2005;23(24):5688–5695. doi:10.1200/JCO.2005.09.021
50. Qin W, Liu K, Su H, et al. Tibial cortex transverse transport promotes ischemic diabetic foot ulcer healing via enhanced angiogenesis and inflammation modulation in a novel rat model. *Eur J Med Res*. 2024;29(1):155. doi:10.1186/s40001-024-01752-4
51. Kong L, Li Y, Deng Z, et al. Tibial cortex transverse transport regulates Orai1/STIM1-mediated NO release and improve the migration and proliferation of vessels via increasing osteopontin expression. *J Orthop Transl*. 2024;45:107–119. doi:10.1016/j.jot.2024.02.007
52. Bahar ME, Kim HJ, Kim DR. Targeting the RAS/RAF/MAPK pathway for cancer therapy: from mechanism to clinical studies. *Signal Transduct Target Ther*. 2023;8(1):455. doi:10.1038/s41392-023-01705-z
53. McCubrey JA, Steelman LS, Chappell WH, et al. Roles of the Raf/MEK/ERK pathway in cell growth, malignant transformation and drug resistance. *Biochim Biophys Acta*. 2007;1773(8):1263–1284. doi:10.1016/j.bbamcr.2006.10.001
54. Axmann A, Seidel D, Reimann T, Hempel U, Wenzel KW. Transforming growth factor-beta1-induced activation of the Raf-MEK-MAPK signaling pathway in rat lung fibroblasts via a PKC-dependent mechanism. *Biochem Biophys Res Commun*. 1998;249(2):456–460. doi:10.1006/bbrc.1998.9188
55. Masson-Meyers DS, Andrade TAM, Caetano GF, et al. Experimental models and methods for cutaneous wound healing assessment. *Int J Exp Pathol*. 2020;101(1–2):21–37. doi:10.1111/iep.12346
56. Yang Y, Li Y, Pan Q, et al. Tibial cortex transverse transport accelerates wound healing via enhanced angiogenesis and immunomodulation. *Bone Jt Res*. 2022;11(4):189–199. doi:10.1302/2046-3758.114.BJR-2021-0364.R1